Minimum Description Length Synthetic Aperture Radar image segmentation

Frédéric GALLAND, Nicolas BERTAUX and Philippe REFREGIER

Abstract— **We present a new Minimum Description Length (MDL) approach based on a deformable partition - a polygonal grid - for automatic segmentation of speckled image composed of several homogeneous regions. The image segmentation thus consists in the estimation of the polygonal grid, or, more precisely, its number of regions, its number of nodes and the location of its nodes. These estimations are performed by minimizing a unique MDL criterion which takes into account the probabilistic properties of speckle fluctuations and a measure of the stochastic complexity of the polygonal grid. This approach then leads to a global MDL criterion without undetermined parameter since no other regularization term than the stochastic complexity of the polygonal grid is necessary and noise parameters can be estimated with maximum likelihood-like approaches. The performance of this technique is illustrated on synthetic and real Synthetic Aperture Radar images of agricultural regions and the influence of different terms of the model is analyzed.**

Keywords— **Image segmentation, Synthetic Aperture Radar, Minimum Description Length, Statistical models.**

I. Introduction

A. Background

SYNTHETIC Aperture Radar (SAR) instruments have been widely used in the past years for remote sensing applications [1]. These microwave active sensors actually offer interesting complementary properties to the classical passive optical systems: they can operate at an time of day, in any weather conditions and offer a high spatial resolution. On the other hand, the speckle [2] effect, inherent to coherent imaging technique, drastically limits the interpretation of the image. A crucial point for SAR image automatic interpretation is the low level step of scene segmentation, *i.e.* the decomposition of the image in a tessellation of uniform areas. Within that domain, a large effort has been done in order to cope with the influence of speckle noise on image segmentation such as edge detection or direct global segmentation.

Edge-based segmentation schemes aim at finding out the transitions between *uniform* areas, rather than directly identifying them. The related algorithms generally work in two stages: they firstly compute an *edge strength map* of the scene and finally extract the local maxima of this map. The first stage is usually achieved using an *edge detection filter*. With SAR images the speckle effect can generally be modeled as a multiplicative noise with a Gamma probability density function (pdf) and edge filters with constant false alarm rate (CFAR) have been developed. Bovik [3] and Touzi [4] defined filters which compute the normalized ratio of averages between two adjacent small regions in an a priori window which is translated on the analyzed image. In the framework of statistical decision theory, Oliver *et al.* determined an optimal filter, based on the likelihood ratio (LR) principle [5]. However, it has been shown [6], [7] that these edge-based detectors introduce a bias and increase the variance in the estimation of the edge position when the window has not the same orientation as the edge (which is the typical practical situation since the edges may have arbitrary orientation in the image). It has also been shown that an efficient technique to refine edge location can be obtained using statistical active contours [6]. But this approach is still far to provide an automatic segmentation procedure. Other approaches such as region growing or region merging [8], [9], [10] have also been developed but they lead to similar limitations.

Global approaches generally consist in optimizing an energy function depending on the whole image. These approaches start from a given model and let it evolve in order to optimize the considered energy criterion.

Many techniques have been proposed for direct global segmentation of SAR images, but because they permit to take into account the noise model, statistical image segmentation techniques have become more and more attractive since the work of Geman and Geman [11]. Markov random fields [12], [13], [14], present many interesting properties. Indeed, they not only allow one to design segmentation techniques which are able to take into account the nature of the speckle noise in a statistically optimal way but they also provide an efficient regularization method. Such regularization is necessary since segmentation is an inverse problem generally ill posed from the mathematical point of view. However, Markov random field models introduce *ad hoc* parameters which cannot be easily automatically determined and which can lead to difficult optimization problem.

Recently, a large interest has been devoted to variational methods for image segmentation [15], [16], [17], [18], [19], [20], [21], [22], [23], [24]. In the case of deformable models, the desirable properties such as continuity and smoothness of the contours are enforced by introducing regularization terms in the functional to optimize. More precisely, this kind of approaches leads to the minimization of an energy-like criterion similar to:

$$E = (1 - \lambda)\ E_{ext}(\mathbf{v}, \mathbf{I}) + \lambda\, E_{int}(\mathbf{v}) \qquad (1)$$

where $E_{ext}(\mathbf{v}, \mathbf{I})$ is an external potential energy which de-

F. Galland, N. Bertaux and P. Réfrégier are with the Physics and Image processing group, Fresnel Institute UMR CNRS 6133, Ecole Nationale Suprieure de Physique de Marseille, Domaine universitaire de St Jerome, 13397 Marseille Cedex 20, France. E-mail: philippe.refregier@fresnel.fr

pends on both the observed image I and the segmentation map $\mathbf{v}$, and $E_{int}(\mathbf{v})$ is an internal energy which allows one to introduce regularization constraints on the segmented image. Regularity properties may correspond for example to smoothness of the contour, penalization of small regions, etc. These approaches require the introduction of parameters, such as for example λ in EQ.(1), which permit to balance between the external potential energy and regularization terms. The value of these parameters may have great influence on the segmentation result and may not be easily predicted by the user. Thus, the situation is analogous to the one obtained with Markov random field approaches.

Recently, deformable models and statistical approaches have been coupled, allowing efficient estimation and regularization of the contours. Whereas some of these methods permit to segment a unique object in the scene ([25], [26], [27], [28], [29], [30]), other are able to segment the scene in several regions ([31]). Based on statistical polygonal snakes, Germain *et al.* [30], [32] proposed a method to correct the bias observed in SAR edge location. However, the extension of this approach to multi region needs an initial segmentation to determine the number of regions and their approximate locations. Furthermore, the fast algorithm developed in [33] and used in this approach was not generalized to non simply connected regions.

Reducing the number of undetermined or free parameters in the criterion to optimize appears as one of the key problems in image segmentation. The Minimum Description Length (MDL) principle, introduced by Rissanen [34], [35] in 1978, has been early used to address this issue. Based on information theory, this principle allows one to estimate the number of needed parameters for parametric description of observed data. The estimation of the values of the parameters are generally obtained using statistical techniques such as maximum likelihood estimation for example. In the context of image segmentation, the estimation of the number of needed parameters for parametric description of observed data can be an interesting alternative to the introduction of regularization terms.

Leclerc [36] proposed very early to apply the Minimum Description Length principle to image segmentation in order to obtain a method without undetermined parameter. The obtained results were illustrated on optical images. Kanungo *et al.* [37] then proposed a MDL merging scheme for multi-band image segmentation leading to a free parameter segmentation method, but which supposes to start with a correct initial over-segmentation. More recently, Zhu and Yuille [31] proposed a region competition algorithm deduced from a MDL criterion. Their approach, combining region growing, region merging and region competition, allows one to segment complex images and provides a general scheme to unify snakes, region growing and Bayesian methods. However, the proposed segmentation algorithm still contains free parameters in the energy criterion which have been introduced in order to obtain better image segmentation. Moreover, the three previous segmentation methods were developed and tested for Gaussian noise and their ability to segment speckle images has not been demonstrated. On the other hand, Figueiredo *et al.* [29] recently demonstrated in the context of snake-based models that the MDL principle can be useful to design a segmentation technique without free parameter and adapted not only to Gaussian but also to Rayleigh noise. More precisely, they proposed to use a MDL method to estimate the order of their contour model, which corresponds to the number of control points of their B-splines contour. They then obtained a global criterion for image segmentation without undetermined parameter and adapted to segment a unique object in the scene. These results have been generalized by Ruch *et al.* [38] in the context of polygonal statistical snake. The MDL criterion introduced previously in [29] has thus allowed them to estimate the number of nodes of the polygonal contour in presence of highly non convex objects in speckle images with a fast and simple algorithm [38].

B. Proposed approach

Applied to image segmentation, the basic idea of the MDL principle consists in finding the image description which has the lowest complexity. The measure of the complexity of a particular image is a difficult problem. In particular, the Kolmogorov complexity of a given image, which corresponds to the length of the smallest program which generates the image, is most of the time uncomputable. Rissanen thus proposed to consider the stochastic complexity which corresponds to the mean number of bits (in the Shannon meaning - see [39]) needed to describe the image with an entropic code. This entropic code is then determined with a probabilistic image model (see [35]).

Our goal in this paper is to propose an automatic image segmentation algorithm adapted to simple speckled SAR images. More precisely, images composed of an unknown number of homogenous speckle fluctuations will be considered. Thus, thanks to this simple image model and based on the MDL principle, one will obtain a global criterion for speckled image segmentation without parameter that needs to be adjusted by the user. Since the MDL criterion corresponds to the stochastic complexity, it depends on a probabilistic model of the image. This approach will thus lead to an algorithm:

1) which does not need *a priori* knowledge on the number of regions,

2) which does not need an initial over-segmentation obtained thanks to another technique,

3) without undetermined parameter in the criterion,

4) adapted to speckle images,

5) and which uses a fast algorithm analogous to the one proposed in [33], but extended to deal with non simply connected regions.

In the proposed approach, the segmentation image model is a polygonal partition, denominated active grid in the following. It is defined as a set of nodes, some of which are joined by segments to delimit regions. The goal of the segmentation algorithm is thus to determine the number of

regions in the image, the number of nodes of the grid and their location in the image. These parameters are obtained by minimizing an appropriate MDL criterion.

In section II, we describe the image model and we determine its stochastic complexity. The precise stochastic complexity for speckled image segmentation degraded by Gamma noise is detailed in the second part of this section. In section III, we propose a simple approach to minimize the stochastic complexity. Starting with an arbitrary regular thin grid, the global optimization procedure is separated in three different procedures which will be used alternatively: a merging procedure where the regions delimited by the grid can be merged, a moving procedure where the nodes of the grid can be moved, and a node's removing procedure to estimate the optimal number of nodes needed in the grid (which is equivalent, from a practical point of view, to a regularization of the contour of the segmented image). Moreover, one will discuss about a fast implementation using contour summation. In section IV, examples of results of the proposed approach on synthetic and real SAR images are presented. We notably show that for simple segmentation purpose like agricultural regions, the above optimization procedure permits one to converge to satisfactory segmentation results and that it also allows one to estimate the speckle order in the image simultaneously.

II. MDL Criterion for image segmentation

A. Determination of the stochastic complexity

Let the image $\mathbf{s}$ be composed of $N = N_x \times N_y$ pixels: $\mathbf{s} = \{\mathbf{s}(\mathbf{x},\mathbf{y}) \,|\, (\mathbf{x},\mathbf{y}) \in [\mathbf{1},\mathbf{N_x}] \times [\mathbf{1},\mathbf{N_y}]\}$ and of R regions Ω_r ($r \in \{1,2...R\}$), each containing N_r pixels. The gray levels of each region Ω_r will be considered as independent random vectors with statistically independent components respectively distributed with a probability density function (pdf) of parameter vector θ_r. Let $\mathbf{w}$ be the function so that $w(x,y) = r$ if and only if the pixel (x,y) belongs to region Ω_r. This function $\mathbf{w}$ - *i.e.* its order R and its values $w(x,y)$ - represents the partition of the image in R regions. So, obtaining this partition function $\mathbf{w}$ can be considered as the purpose of an image segmentation technique. We propose to implement this partition $\mathbf{w}$ with a polygonal grid - a set of nodes linked by segments - in order to define boundaries of regions. Let us note that to define $\mathbf{w}$ thanks to a polygonal grid, we adopt the convention developed in [32], *i.e.* the partition grid is translated by $(1/2, 1/4)$ with respect to the pixel grid, so that the grid defines regions without ambiguity.

In order to apply the MDL principle, let us now estimate the stochastic complexity, or in other words, the mean code length of the whole image description with a given partition function $\mathbf{w}$. The number of bits necessary to encode the image is composed of two terms: the sum $\Delta_S = \sum_{r=1}^{R} \Delta_r$ of the total number of bits Δ_r needed to describe the pixel's gray levels in each region Ω_r with an entropic code [39] and the length of the grid description.

Let us first determine the number of bits needed to encode the pixels' gray levels of a given region Ω_r, knowing the partition $\mathbf{w}$. To encode the gray levels in the region Ω_r composed of N_r pixels, one first needs to encode the parameter vector θ_r of the pdf P_{θ_r} in this region and then to encode the gray levels of the pixels of this region. Let α be the dimension of the parameter vector[1]: so, one has to encode α scalar parameters. Since each of them are estimated on a sample of N_r pixels, an approximation of the code length associated to the parameter vector is $\alpha log_2 \sqrt{N_r}$ (*cf.* [35]). Knowing the pdf parameter vector, the average code length of an entropic code of the pixels' gray levels of region Ω_r is given by (*cf.* [39]):

$$-l_2[\Omega_r|\theta_r] = -\sum_{(x,y)\in\Omega_r} log_2[P_{\theta_r}(s(x,y))] \qquad (2)$$

where the base 2 log-likelihood has been used.

One finally obtains $\Delta_r = \frac{\alpha}{2} log_2 N_r - l_2[\Omega_r|\theta_r]$ and so for the whole image:

$$\Delta_S = \sum_{r=1}^{R} \left(\frac{\alpha}{2} log_2 N_r - l_2[\Omega_r|\theta_r] \right) \qquad (3)$$

The determination of the code length Δ_G of the grid is less straightforward. Two nodes of the grid will be said neighbors if there exists a unique segment of the grid which links them. We will also define a segment vector as the vector which links the current node to the corresponding neighbor node. The coordinates of the segment vector are thus the difference between the coordinates of the neighbor node and the coordinates of the current node.

Only some particular graphs can be drawn continuously - *i.e.* without jump between non neighbor nodes - and with passing one and only one time by all the segments: they correspond to Eulerian graphs. In the particular case of Eulerian graphs, an obvious coding method of the grid may consist in coding the coordinates of a starting node and then in successively encoding the coordinates of the segment vectors so that the grid has been drawn continuously by meeting one and only one time each segment. In the general case of non Eulerian graph, this procedure will not be applicable without making jumps between non neighbor nodes. A simple way to describe the grid can thus be obtained as follows:

1) choose a starting node and code its coordinates in the image,

2) encode the coordinates of the segment vector formed by the current node and one of its neighbor nodes (the segment vector corresponds to a segment of the grid),

3) then, consider this neighbor node as the current node and go to **(2)** until no segment has to be encoded twice,

4) when no segment vector coding is possible on the grid without encoding twice the same segment, specify - just after having given the coordinates code of the starting node - the number of segments which have been encoded and then jump to another starting node (*i.e.* go to **(1)**),

[1]For example, for a gamma law we have $\alpha = 1$ (the only parameter is the mean) and for a Gaussian law, $\alpha = 2$ (the 2 parameters are the mean and the variance).

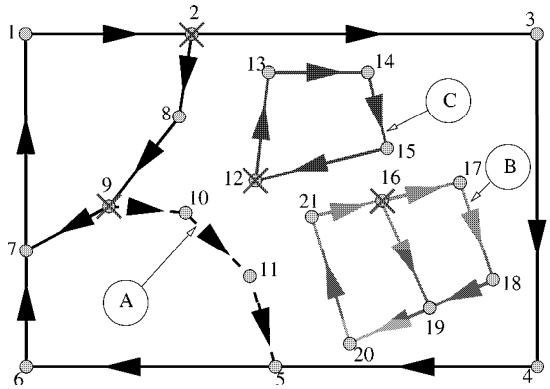

Fig. 1. *Minimum number of starting points needed to describe a grid. To meet one time - and only one - each segment, one travels around the followings nodes: (2, 3, 4, 5, 6, 7, 1, 2, 8, 9, 7) then (9, 10, 11, 5) then (16, 17, 18, 19, 20, 21, 16, 19) and finally (12, 13, 14, 15). So the number of starting nodes - marked with a cross - is* $n = 4$. *These starting nodes include* $n_{ON}/2 = 3$ *odd nodes (2, 9 and 16) and one even node (12) which leads to the only simply connected component of the graph without any odd node (C).*

5) continue until all the segment vectors have been encoded.

Let us now determine the minimum number n of starting nodes (*i.e.* of jumps) which are needed to draw the grid by passing one and only one time by all the segments (thus $n = 1$ for an Eulerian graph). A node with an odd number of segments starting from it (denominated an odd node in the following) must be either a starting or an arrival node, when one wants to encode the segments of the grid with a minimum number of jumps (*cf* Fig.1). In that case, the number of starting nodes has to be equal to half the number of odd nodes, noted n_{ON}. However, for each simply connected graph, the coordinates of a starting node has also to be specified. Let n_{SC} be the number of simply connected components without odd node. One then obtains:

$$n = \frac{n_{ON}}{2} + n_{SC} \tag{4}$$

Since there are N pixels in the image, the location of a node will then be coded with $log_2 N$ bits. Let p denote the number of segments of the grid. Given a starting node, one must encode the number of segments that will be continuously encoded before a jump. This number can vary between 1 and p, needing at most $log_2 p$ bits. Then to encode the list of connected segments (*i.e.* the coordinates of the vector formed by neighbor nodes) one will have to encode p segment vectors since each segment will be encoded one and only one time.

It is clear that coding the segment vector coordinates of neighbor nodes can be performed by using $log_2 N$ bits. However, it is far to be an appropriate estimation of the minimum mean number of bits which are necessary. A better approximation can be obtained using a Shannon code of the segment vector coordinates of neighbor nodes. However, for determining such a Shannon code, one needs to determine the underlying probability distribution of the vector coordinates of neighbor nodes. Let $d_x(i)$ and $d_y(i)$ be the absolute value of the horizontal and vertical coordinates of the segment vector number i: $d_x(i) = |x_2(i) - x_1(i)|$ and $d_y(i) = |y_2(i) - y_1(i)|$ where (x_1, y_1) and (x_2, y_2) are the coordinates of the extremities of the segment number i. One supposes that $d_x(i)$ (resp. $d_y(i)$) is distributed with a pdf $P_{m_x}(d)$ (resp. $P_{m_y}(d)$) with m_x (resp. m_y) the parameter of the pdf. Since both $d_x(i)$ and $d_y(i)$ will play equivalent role in the following, x or y index will not be noted unless necessary. Knowing the parameter m of the pdf $P_m(d)$, the average code length needed to encode the p horizontal or vertical components of the segment vectors can be approximated by the negative of the base 2 log-likelihood $l_2[\chi|m]$ with $\chi = (d(i))_{i\in[1,p]}$. However, since d is in fact the absolute value of the abscissa or the ordinate, to encode the p segment vectors' horizontal or vertical components, p bits of sign have to be added to the log-likelihood. So the Shannon code length of the whole grid is:

$$\begin{aligned}\Delta_G &= n(log_2 N + log_2 p) - l_2[\chi_x|m_x] \\ &\quad -l_2[\chi_y|m_y] + 2p + \Delta_2(m_x) + \Delta_2(m_y)\end{aligned} \tag{5}$$

where $\chi_x = (d_x(i))_{i\in[1,p]}$ and $\chi_y = (d_y(i))_{i\in[1,p]}$ and where $\Delta_2(m_x)$ and $\Delta_2(m_y)$ are the number of bits needed to encode the parameters m_x and m_y. According to [35], since m_x and m_y are estimated on a p-sampling, each one can be encoded in $log_2\sqrt{p}$ bits. For simplicity reasons, let us now consider natural logarithms log instead of the base 2 logarithms log_2. The length coding are thus measured in nats instead of bits, leading to:

$$\begin{aligned}\Delta_G &= n(log\, N + log\, p) - l_e[\chi_x|m_x] \\ &\quad -l_e[\chi_y|m_y] + 2p\, log\, 2 + log\, p\end{aligned} \tag{6}$$

where $l_e[.]$ denotes the log-likelihood expressed with natural logarithms.

In order to determine an appropriate pdf $P_m(d)$, we propose to apply the maximum entropy principle with the constraint that the statistical mean value is assumed known. In other words, one determines the pdf P which maximises the entropy $S = -\int_0^{+\infty} P(x) \log P(x)\, dx$ with the constraint that its mean is equal to m: $\int_0^{+\infty} x\, P(x)\, dx = m$. The obtained corresponding pdf is thus an exponential law:

$$P_m(d) = \frac{1}{m} e^{-\frac{d}{m}} \tag{7}$$

where m is the statistical mean value. Then one gets:

$$l_e[\chi|m] = \sum_{i=1}^{p} log\left[P_m(d(i))\right] \tag{8}$$

and replacing m by its ML estimate $\widehat{m} = \frac{1}{p}\sum_{i=1}^{p} d(i)$, one obtains:

$$l_e[\chi|\widehat{m}] = -p\, log(\widehat{m}) - p \tag{9}$$

The code length to encode the grid is then deduced from (6):

$$\begin{aligned}\Delta_G &= n(log\, N + log\, p) + log\, p \\ &\quad +p(2 + log(2\widehat{m_x}) + log(2\widehat{m_y}))\end{aligned} \tag{10}$$

where $\widehat{m_x} = \frac{1}{p}\sum_{i=1}^{p} d_x(i)$ and $\widehat{m_y} = \frac{1}{p}\sum_{i=1}^{p} d_y(i)$.

In conclusion, one proposes to evaluate the stochastic complexity of the image using a particular segmentation (*i.e.* a particular grid) by:

$$\begin{aligned}\Delta &= n(log\, N + log\, p) + log\, p \\ &\quad + p(2 + log(2\widehat{m_x}) + log(2\widehat{m_y})) \\ &\quad + \sum_{r=1}^{R}\left(\tfrac{\alpha}{2} log\, N_r - l_e[\Omega_r|\theta_r]\right)\end{aligned} \tag{11}$$

Since the log-likelihood of the image

$$l_e\left[\mathbf{s}|\mathbf{w}, (\theta_\mathbf{r})_{\mathbf{r}\in[\mathbf{1},\mathbf{R}]}\right] = \sum_{r=1}^{R} l_e[\Omega_r|\theta_r] \tag{12}$$

has to be specified in order to determine the stochastic complexity Δ, this criterion can be adapted to the gray level pdf of the image. This is the object of the next section.

B. Determination of the log-likelihood

The classical model to describe speckle fluctuation (see [2]) is to describe the gray level fluctuation by a Gamma law of order L which pdf is:

$$P_\theta(x) = \frac{L^L}{\theta^L\,\Gamma(L)} x^{L-1} e^{\frac{-L\,x}{\theta}} \tag{13}$$

where θ is the statistical mean value. The log-likelihood in the region Ω_r is then:

$$\begin{aligned}l_e[\Omega_r|\theta_r] &= N_r\,(L\,log\,L - L\,log\,\theta_r - log\,\Gamma(L)) \\ &\quad -\tfrac{L}{\theta_r}\textstyle\sum_{(x,y)\in\Omega_r} s(x,y) \\ &\quad +(L-1)\textstyle\sum_{(x,y)\in\Omega_r} log\,(s(x,y))\end{aligned} \tag{14}$$

The ML estimate $\widehat{\theta}_r$ of θ_r is thus the simple sufficient statistic of the gamma law:

$$\widehat{\theta}_r = \frac{1}{N_r}\sum_{(x,y)\in\Omega_r} s(x,y) \tag{15}$$

Replacing θ_r by $\widehat{\theta}_r$ in EQ.(14),one obtains:

$$\begin{aligned}l_e\left[\mathbf{s}|\mathbf{w}, \left(\widehat{\theta}_\mathbf{r}\right)_{\mathbf{r}\in[\mathbf{1},\mathbf{R}]}\right] &= N\,L\,log\,L - L\textstyle\sum_{r=1}^{R} N_r\,log\,\widehat{\theta}_r \\ &\quad -N\,log\,\Gamma(L) - N\,L + (L-1) \\ &\quad \times\textstyle\sum_{(x,y)\in Image} log\,(s(x,y))\end{aligned} \tag{16}$$

where $l_e\left[\mathbf{s}|\mathbf{w}, \left(\widehat{\theta}_\mathbf{r}\right)_{\mathbf{r}\in[\mathbf{1},\mathbf{R}]}\right] = \sum_{r=1}^{R} l_e\left[\Omega_r|\widehat{\theta}_r\right]$.

In this expression, one can note that only $-L\sum_{r=1}^{R} N_r log\widehat{\theta}_r$ will vary for different partitions (*i.e.* segmentations) of the image. Thus, the log-likelihood can be written

$$l_e\left[\mathbf{s}|\mathbf{w}, \left(\widehat{\theta}_\mathbf{r}\right)_{\mathbf{r}\in[\mathbf{1},\mathbf{R}]}\right] = -L\sum_{r=1}^{R} N_r\,log\,\widehat{\theta}_r + K(L) \tag{17}$$

with $K(L)$ independent of the segmentation result but is dependent on L.

The log-likelihood for other statistical laws belonging to the exponential family have been determined in [33] for the statistical snake technique and could be generalized for the segmentation method proposed here.

III. MDL SEGMENTATION

A. General algorithm

Once the description length, measured by the stochastic complexity Δ - also called MDL criterion in the following - associated to a given grid for a specific image has been determined, the segmentation problem consists in finding the partition function $\mathbf{w}$, or in other words, the grid which minimizes the criterion Δ. The segmentation problem is thus an optimization problem and the variable is the partition grid *i.e.* the region labeling, the number of nodes of the grid and their location in the image. For this purpose, we propose a simple approach which consists in alternatively optimizing the region labeling with a merging procedure, the nodes' number k with a removing method and the location of the nodes with a moving technique.

Let us now briefly describe these three different optimization procedures.

B. Regions' merging

To find the region labeling, a merging scheme can be implemented. The principle is quite simple: two neighboring regions Ω_A and Ω_B are merged if this merging leads to a decrease of the stochastic complexity Δ. The stochastic complexity of EQ.(11) can be rewritten:

$$\Delta = F - \sum_{r=1}^{R} l_e[\Omega_r|\theta_r] \tag{18}$$

where $F = \Delta_G + \frac{\alpha}{2}\sum_{r=1}^{R} log\,N_r$ and Δ_G given by EQ.(10). Let us denote Δ and F (resp. Δ' and F') these values before (resp. after) merging and θ_{AB} the parameter vector of the region $\Omega_{AB} = \Omega_A \bigcup \Omega_B$. Ω_A and Ω_B are merged when $\Delta' - \Delta < 0$, *i.e.* when

$$l_e[\Omega_A|\theta_A] + l_e[\Omega_B|\theta_B] - l_e[\Omega_{AB}|\theta_{AB}] < S \tag{19}$$

where $S = F - F'$. One can remark that this test is similar to a Generalized Likelihood Ratio Test (GLRT)[40] with a threshold S determined thanks to the MDL criterion Δ. In order to allow a graduated convergence, in the following, one may combine two GLRT approaches, one with a threshold $S = F - F'$ obtained with the MDL criterion Δ and an other with an *ad hoc* threshold $\widetilde{S}$. We will show in section IV-C that this *ad hoc* procedure is not absolutely necessary. Indeed, a simpler procedure which only uses a MDL region merging can be implemented when the speckle order L is also estimated.

C. Nodes' moving

The obtained grid after a merging - as well as with the initial grid - may contain regions which are not homogeneous. In other words, a region of the grid may contain different parts of regions of the image (*i.e.* with different reflectivity). Instead of considering a splitting procedure which may lead to very small regions and then to difficult statistical tests, we propose to implement a moving procedure. This moving approach allows one to move a node

in order to minimize the MDL criterion Δ. The advantage of this method is that at each step of the algorithm, one deals with regions of sufficiently large pixel numbers, which is more reliable than using regions with very small pixel numbers.

This procedure is similar to the one presented in [32] and will not be detailed here. It simply consists in considering successively each node of the grid and in randomly moving it: the move is accepted if it has lowered the MDL criterion Δ, otherwise it is canceled.

D. Nodes' removing

Since the grid may have many parameters (essentially the coordinates of the nodes), the segmentation task is an ill posed problem. As a consequence, the minimization of the MDL criterion Δ with a very large number of nodes leads to very fluctuating boundaries. A classical approach in that context consists in regularizing the solution by adding to the criteria a Tikhonov-like regularization term, such as an elastic energy penalization analogous to the one used in variational approaches [17], [41], [21]. However these regularization techniques present many drawbacks in our context. The first one is that it introduces *ad hoc* parameters which cannot be easily estimated. The second one is due to the fact that the moving and the merging procedures are driven by the minimization of the MDL criterion Δ. Then if the grid contains more nodes than necessary, one will obtain an overestimation of the grid complexity Δ_G and thus an erroneous segmentation result.

We thus propose to implement a removing step which is very simple from an algorithmic point of view. It simply consists in scanning each double connected node of the grid and suppressing it if this allows to decrease the MDL criterion Δ. However, in order to obtain a graduated removing procedure in the proposed implementation, we first determine the MDL decrease involved by the suppression of respectively each node of the grid, and then suppress the one which leads to the most important decrease. This procedure is analogous to the one presented in [38] in the context of the statistical snake.

E. Global optimization and fast implementation

Since for the three above optimization procedures, the most computational task is to determine the sufficient statistics $\widehat{\theta}_r$ of EQ.(15), each step can be very time consuming. We thus propose to generalize and to implement a fast algorithmic approach which consists in substituting to the surface summation of the gray levels in EQ.(15), a contour summation on a preprocessed image. The proposed approach is analogous to the one described in [33], [32] and has been generalized in order to deal with non simply connected regions. This generalization is discussed in appendix A.

In order to apply the previous optimization procedure, one has to start with an initial grid. In the following we consider rectangular initial grid but other choices - maybe more suited to grid dynamics - could have been considered. Since our goal in the following will be to illustrate the robustness of the proposed MDL segmentation technique, this suboptimal choice of the initial grid also contributes to this purpose. The final segmentation is obtained when the MDL criterion cannot decrease anymore. More precisely, the region merging and node removing optimization procedures are stopped when no further minimization of the stochastic complexity can be obtained. There is thus no need of *ad hoc* parameter for stopping these optimization algorithms. Of course, during the node moving optimization, it is not possible to explore all the possible moves exhaustively in a reasonnable time: the user has thus to fix the number of iterations of the process.

IV. EXPERIMENTAL RESULTS

In this section, we illustrate the results of the proposed segmentation technique obtained with some synthetic and real SAR images.

As mentioned above the MDL threshold $S = F - F'$ used in the merging algorithm depends on the nodes' number and favors merging if this nodes' number is large which may result in an irreversible under-segmentation. To overcome this problem, we first propose to alternate the three above optimization procedures without directly applying the MDL threshold for region merging in the first step of the optimization. More precisely, a GLRT merging scheme with a fixed threshold (chosen equal to 3 for all the following experimental results) is applied in order to reduce the region's number. After this merging procedure, a moving optimization and a node's removing optimization are performed. Since node's removing have slightly modified the shape of the grid, another moving optimization is applied. Then, with this reduced number of nodes, another sequence of region merging, but now with the MDL threshold, followed by a moving and a node's removing optimization is applied. It is worth noting that, although the optimization procedure may contain *ad hoc* parameters (as most numerical optimization methods), the segmentation is obtained by minimizing the parameter free MDL criterion Δ. A simpler approach will be proposed in section IV-C when the speckle order L is also estimated.

A. Synthetic image

According to this optimization process, we first present our results on synthetic images with speckle noise. The first image (*cf.*FIG.2) is a 256×256 pixel synthetic image with speckle noise of order 1. This image is analogous to the agricultural SAR image of FIG.5. The second one (*cf.* FIG.3 - upper line) is composed of 9 homogeneous regions with different contrasts[2] varying from 2 to 18. Its size is 595×765 pixel and it also presents a speckle noise of order 1. The third one (*cf.* Fig.3 - lower line) is a target's synthetic image of 256×256 pixels presenting a first order speckle phenomenon with a contrast equal to 4 and notably permits to demonstrate the ability of the algorithm to deal with non simply connected regions (*cf* appendix A).

[2]We remind that in speckle images, the contrast between two regions is defined by the ratio of their means.

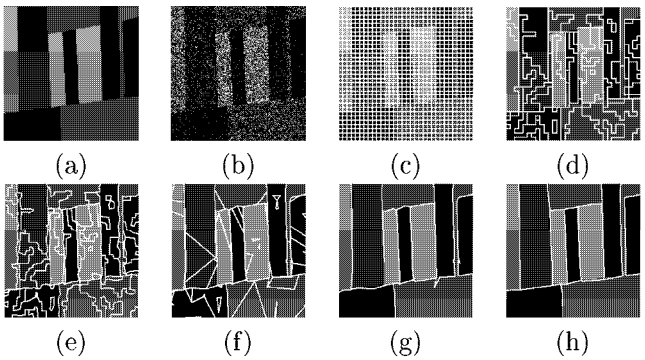

Fig. 2. *Segmentation of a* 256×256 *pixels synthetic image with a first order speckle noise and analogous to the real SAR image of* FIG.5. ***(a)-(b)*** *Synthetic image without and with noise - **(c)** Initial grid delimiting regions of size* 8×8 *pixels - **(d)** After a region merging with GLRT criterion (threshold 3) - **(e)** After a move of the grid - **(f)** After a nodes' removal and a move of the grid - **(g)** After a region's merging with the MDL criterion - **(h)** Final segmentation after a last move of the grid and a last nodes' removal. Although the results are superposed to the non noisy image for visualization purpose, the processed image at each step is* FIG.***(b)***.

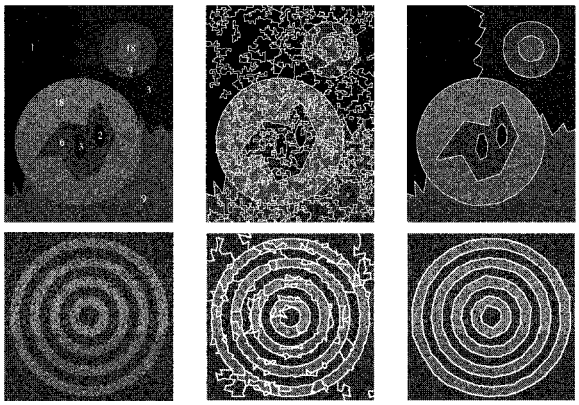

Fig. 3. *Segmentation of synthetic images. Upper line: synthetic image (*595×765 *pixels) composed of 9 regions with speckle noise of first order. Bottom line: target (*256×256 *pixels) with speckle noise of first order and a contrast equal to 4. From left to right: **(a)** synthetic images (the written numbers represent the mean in each region). The initial grid delimits regions of size* 8×8 *pixels. **(b)** Grid after a merging (threshold 3) and a moving. **(c)** Final segmentation after a nodes' removing, a moving, a merging with MDL threshold, a moving and a last nodes' removing. Let us note that the images' gray levels have been modified to be better visualized.*

The segmentation time for the 256×256 pixel images of FIG.2 and Fig.3 (lower line) is less than 6 seconds on a standard PC (Pentium III,800 MHz), but one must point out that the algorithm has not yet been optimized to reduce this computation time.

B. SAR images

Let us now present results on real SAR images (see FIG.4, FIG.5 and FIG.6). For all these examples, the segmentation process is the same and one can see that this MDL segmentation algorithm provides very interesting results, although it is automatic. However, this technique may probably be unappropriated for more complex images as urban areas.

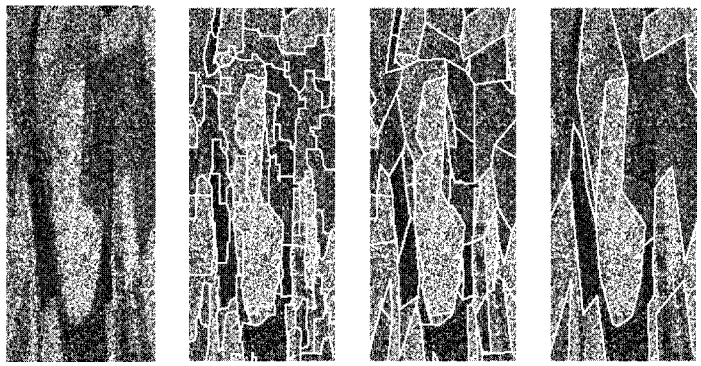

Fig. 4. *Extract (*150×350 *pixels) of a single look SAR image of an agricultural area near Bourges (France) obtained by the ERS-1 satellite (distributed by the ESA and provided by the CNES). **(a)** Original image. The initial grid delimits regions of* 8×8 *pixels. **(b)** After a merge with GLRT criterion (threshold is equal to 3) and a move. **(c)** After a nodes' removing and a move. **(d)** Final segmentation after a merging with MDL threshold, a moving and a last nodes' removing.*

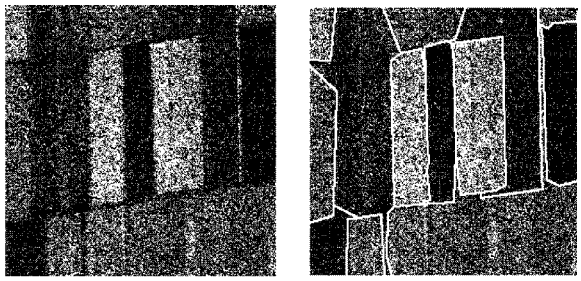

Fig. 5. *Extract (*250×250 *pixels) of a single look SAR image of agricultural area in Ukraine obtained by the ERS-1 satellite (distributed by the ESA and provided by the CNES). **(a)** SAR image. The initial grid delimits regions of* 5×5 *pixels. **(b)** Final segmentation.*

As a conclusion, one has to emphasize that, in order to minimize the MDL criterion Δ, three kinds of optimization procedures have to be implemented (merging, moving and nodes' removing). However, a MDL merging optimization implemented before a nodes' removing procedure will lead to too many regions' merging. Thus, the results of these three optimization schemes are not independent and alternative optimizations have to be performed so that the segmentation result does not correspond to an unsatisfactory local minimum of the MDL criterion.

C. Robustness

C.1 Influence of the choice of the pdf of the pixels' gray levels

Let us first analyze the influence of the choice of the pdf in the image model on the segmentation result. For that purpose, the test image of FIG.3 (upper line) presenting a gamma noise of first order is segmented first by minimizing the MDL criterion designed for gamma pdf of order 1 (see FIG.7-a) or by minimizing the MDL criterion designed for

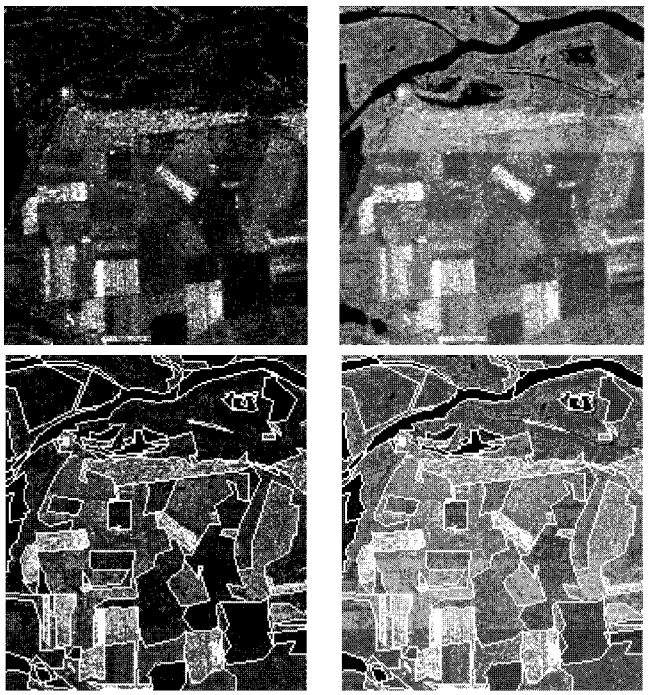

Fig. 6. *Extract (171×190 pixels) of a SAR image in Ukraine obtained by the ERS-1 satellite (distributed by the ESA and provided by the CNES) and composed of agricuktural areas, lakes and rivers. Line 1: SAR image (on the left) and the same image after having modified the pixel gray levels in order to better visualized the image (on the right). Line 2: segmentation result displayed on the first line images. In order to be able to detect thin rivers, the initial grid has regions of 3 × 3 pixels.*

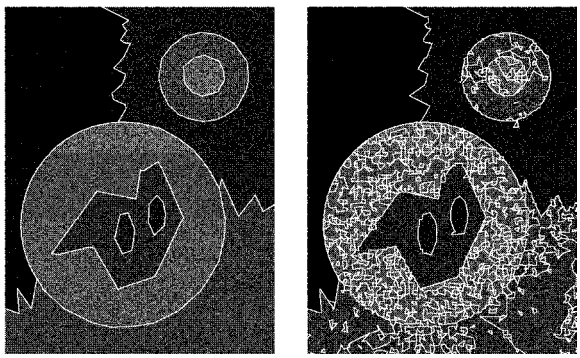

Fig. 7. *Influence of the gray level pdf used in the model: segmentation of a synthetic image, whose gray level statistics is a first order speckle noise. Segmentation results with the following model: gamma of order 1 (a) and Poisson (b).*

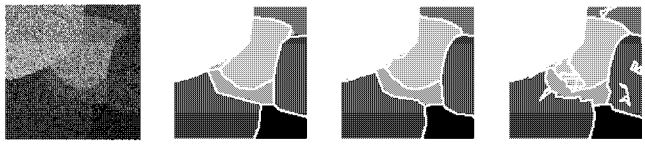

(a) (b) (c) (d)

Fig. 8. *Influence of the order of the gamma pdf: segmentation of the test image (a) whose gray level are distributed with third order speckle noise. Results with the gamma pdf order set to 1 (b), 3 (c) and 10 (d). For visualization purpose, the segmentation results are superposed to a noise-free image.*

a Poisson pdf (see FIG.7-b) whose likelihood is (*cf.* [33]):

$$-\sum_{r=1}^{R} N_r \, \widehat{\theta}_r \, log\left(\widehat{\theta}_r\right) + K' \qquad (20)$$

where $\widehat{\theta}_r = \frac{1}{N_r} \sum_{(x,y)\in\Omega_r} s\,(x,y)$ and K' a constant which has no influence on the segmentation result. The results presented on FIG.7 clearly show that the choice of the pdf is fundamental in that case, in particular to estimate correctly the number of regions.

C.2 Influence of wrong speckle order choice

In the previous examples, the order L of the gamma pdf was assumed to be a priori exactly known. We propose to analyze here the influence on the segmentation results, of an erroneous choice of the speckle order L for the likelihood term in the MDL criterion Δ. For that purpose a synthetic speckled image (128 × 128 pixels) of order 3 has been generated. Then, considering always the same optimization process, different MDL segmentations have been obtained with respectively MDL criterion determined for gamma law of order 1, 3 and 10. Results are shown on FIG.8.

One can see on FIG.8-d that the segmentation result obtained with a speckle order equal to 10 (*i.e.* higher than the speckle order of the image) for the likelihood term in the MDL criterion, leads to an over estimation of the numbers of nodes and regions in the final grid. On the other hand, the segmentation result obtained with a speckle order equal to 1 (*i.e.* lower than the speckle order of the image) leads to a grid with too many removed nodes (see FIG.8-b). Moreover, one can see that the best result is obtained with the true speckle order, *i.e.* $L = 3$ (FIG.8-c).

These results can be easily interpreted when one analyzes EQ.(17). Indeed, the speckle order L is a multiplicative term on the likelihood part of the MDL criteria Δ. Thus, when L is high the coding part of the grid Δ_G has less influence than with low L values.

C.3 Segmentation without knowledge of the speckle order

When the order of the gamma law of the speckle fluctuations is not known, it is still possible to use the stochastic complexity in order to segment the image. In this case, the order L is considered as a nuisance parameter since the segmentation result is the parameter of interest. One approach would have been to estimate the order L in the Maximum Likelihood meaning. Although no explicit equation of this estimate of L can be rigorously obtained, one can either consider some approximations or use an iterative approach. Another solution is to determine the stochastic complexity for different values of L and then to choose the one which minimizes the MDL criterion (which is equivalent to maximize the Maximum Likelihood criterion). Since this method is more specific to our approach, this is the one we propose to discuss. Because the dynamic of the grid is essentially a simplification procedure, we first apply a MDL segmentation with a large order (typically 10 in the follow-

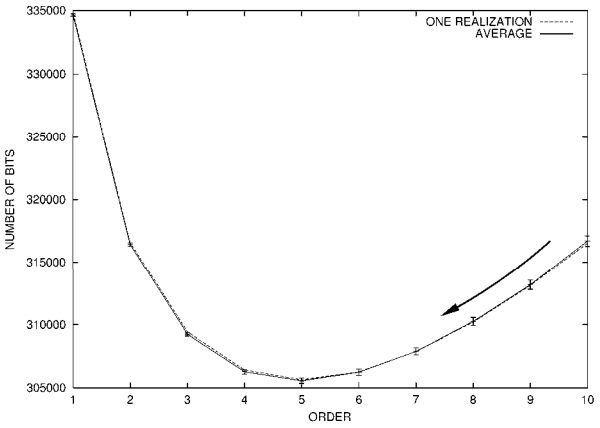

Fig. 9. *Estimation of the speckle order: evolution of the MDL criterion. The segmentation is performed on the synthetic image of* FIG.*2 corrupted with a 5-order speckle noise. The initial grid delimits regions of size* 8×8 *pixels. Several segmentations are performed by minimizing the MDL criterion designed for a gamma law of order 10, 9, 8, etc, and finally of order 1. At each step, the previous segmentation result is used as the new initial grid. This curve presents the evolution of the MDL criterion when the order in the MDL criterion* Δ *vary from 10 to 1: the smallest stochastic complexity corresponds to the real order, i.e.* $L = 5$*. The dashed curve is obtained for one realization whereas the solid curve represents the average of 100 realizations of this experiment. One must point out that the true value (i.e.* $L = 5$*) always correspond to the minimum.*

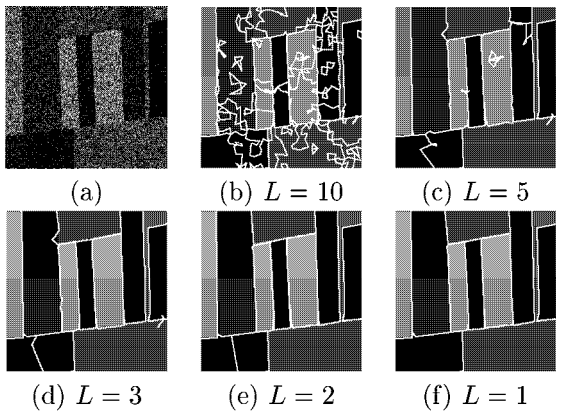

Fig. 10. *Estimation of the speckle order: segmentation results. The segmentation is performed on the synthetic image of* FIG.*2 corrupted with a 2-order speckle noise* ***(a)****. The initial grid delimits regions of size* 8×8 *pixels and the segmentation is first performed when the gamma law order* L *is set equal to 10 in the computation of the MDL criterion* Δ*. The segmentation result for the current order* L *is then used as initial grid to segment the image with an order set to* $L-1$*. So, the set order decreased by 1 at each step and it varies from 10 to 1. The* FIG.***(b)-(c)-(d)-(e)-(f)*** *present the obtained results with orders respectively set to 10, 5, 3, 2, 1. For this numerical experiment, the stochastic complexity is minimal when* $L = 2$*, which also corresponds to the best segmentation result as it can be observed in this figure (one must note that the 2 small regions on the left bottom corner present a very few contrast (1.2) and are merged when* L *is set to 1).*

ing experiments). When the segmentation is obtained with the current order L, the obtained polygonal grid is considered as the initial grid for a new MDL segmentation with a Stochastic complexity criterion determined with order $L-1$. These iterations are stopped when $L = 1$. The estimated order is then chosen as the one which has lead to the smallest stochastic complexity[3] and the corresponding segmentation is considered as the proper one (*cf.* FIG.9 and 10).

Since the imposed order L in the stochastic complexity Δ now slowly decreases, the segmentation is more robust with respect to the optimization scheme. Indeed the influence of the stochastic complexity of the grid relatively to the one of the gray levels is introduced gradually and there is now no need to perform alternative optimizations such as the ones described in section IV-A and IV-B. Thus, at each step of this new segmentation procedure, *i.e.* at each order, one only performs a merging optimization with the MDL threshold (no GLRT optimization is thus anymore implemented), a moving optimization and a nodes removing optimization. This procedure thus permits to find efficiently the speckle order (*cf.* FIG.9), it provides good segmentation results (*cf.* FIG.10) and it is more robust to the optimization strategy with only a small increase of the computational time (typically the computational time has only been multiplied by a factor less than 2).

[3]One must note that in order to compare the stochastic complexity Δ for different order, one must use EQ.(16) instead of EQ.(17), since K depends on the order L.

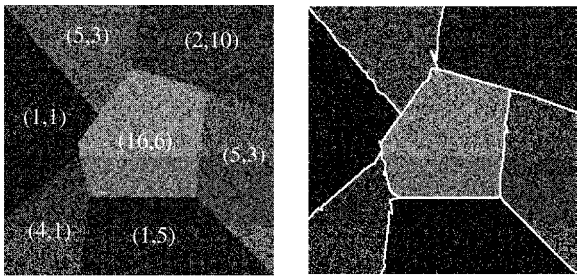

Fig. 11. *Segmentation of a K-law speckled synthetic image. The synthetic image corrupted with a K-law single look is presented on* FIG.***(a)****. In each region,* (m, σ) *gives the mean* m *and the texture parameter* σ *(small values of* σ *correspond to high textured regions; for untextured regions,* $\sigma = \infty$*). The segmentation procedure is analogous to the one presented in* FIG.*10: the initial grid delimits regions of size* 8×8 *pixels and several segmentations are performed with an order set to 10, 9, 8, ..., 1. At each step, the previous segmentation result is used as the new initial grid. The proper segmentation is considered to be the one with the smallest stochastic complexity:* FIG.***(b)*** *presents the segmentation obtained in that case.*

C.4 Segmentation of K-law speckled images

Some SAR images may have speckle fluctuations which are better described with K-law [42], [43], [44] than with Gamma laws. K-laws are generally the consequence of strong inhomogeneity of the underlying reflectivity of the scattering regions. We report in FIG.11 an example of segmentation result which can be obtained when the procedure of the previous section is applied to such a speckle image. One can observe that the segmentation quality is still correct.

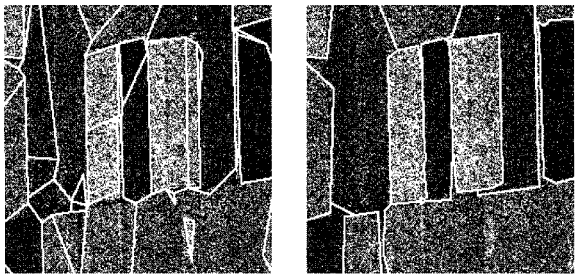

Fig. 12. *Influence of the choice of the grid code length: segmentation result on the SAR image of* FIG.5 *with* $\Delta_G = k \log N$ *(on the left) and with the* Δ_G *found in* EQ*(6) (on the right).*

C.5 Influence of the choice of the grid code length estimation method

Let us now illustrate the influence of the stochastic complexity (*i.e.* the code length) Δ_G of the grid. On FIG.12, we compare the segmentation result when two different expression of the grid code length are used: the expression Δ_G defined by EQ.(6) and another one, analogous to the ones presented in [29], [38] and equal to $k \log N$ where k is the number of nodes. One can see that this term has a great influence on the final segmentation: when $\Delta_G = k \log N$, the number of nodes and regions are most of the time overestimated.

V. CONCLUSION

We have proposed a new Minimum Description Length (MDL) approach based on a polygonal grid partition of the image for automatic segmentation of speckled image composed of several homogeneous regions. The segmentation is obtained from an initial polygonal grid and by minimizing the MDL criterion considering three kinds of evolution of the grid: merging of regions of the grid, removing of nodes of the grid and deformation of the grid by moving its nodes. The proposed MDL criterion takes into account the probabilistic properties of speckle fluctuations and a measure of the stochastic complexity of the polygonal grid. This approach then leads to a criterion without undetermined parameter: noise parameters can be estimated with maximum likelihood like approaches and regularization of the segmentation does not require additional regularization terms involving undetermined parameters. The results showed that this segmentation technique is efficient for Synthetic Aperture Radar images (SAR) of agricultural regions. Although SAR images are strongly noisy, it has been demonstrated that the proposed approach can be considered as automatic and robust provided that correct models have been considered for the speckle fluctuations and the measure of the polygonal grid stochastic complexity. Furthermore, a fast implementation which generalized the technique proposed in [33] has also been proposed.

Of course many questions are still open and the proposed technique offers many new perspectives of research. First of all, it would be interesting to study the generalization of this approach to other kind of noise, such as additive Gaussian noise for video images or Poisson noise for medical or astronomical images. In the proposed model, the regions are assumed homogeneous (this is also a classical assumption with Markov random field approaches). It would be interesting to study if this constraint can be easily relaxed and, in particular, if one can preserve a fast implementation which allows one to substitute surface summations by contour summations. More generally, the proposed technique opens new questions on the optimization procedures needed for the minimization of the stochastic complexity. Indeed, the optimization has to be performed on different heterogeneous variables (region labels, number on nodes, location of nodes) and there is presently no proof of the convexity of the criterion. On the other hand, the experimental results of this paper show that a simple optimization technique can lead to very good results without requiring simulated annealing or other slow optimization techniques useful for very highly non convex criteria.

ACKNOWLEDGMENTS

The authors are grateful to the French Spatial Agency (CNES) which supplied the SAR data and to F. Goudail for fruitful discussions and suggestions.

APPENDIX

I. CONTOURS' SUMMATION ADAPTED TO NON CONNECTED REGIONS

In this appendix, we present a generalization of the fast algorithm presented in [33], [32] to non simply connected regions.

In order to estimate the number of pixels and the parameter vector θ_r of the pdf in each region Ω_r, one has to determine

$$I_k(\Omega_r) = \sum_{(x,y)\in\Omega_r} s^k(x,y) \tag{21}$$

with $k = 0$ or 1. One can substitute the 2D summation over a region Ω_r by a 1D summation over its contour by implementing a fast algorithm approach analogous to the one developed in [33] and adapted to an active grid in [32]. Since the computation of $\widehat{\theta}_r$ is very fast with this procedure, it is possible to always use the exact value of $\widehat{\theta}_r$ in the optimized criterion, *i.e.* $\widehat{\theta}_r$ is updated at each modification of the grid. However, since up to now this algorithm was only presented for simply connected regions, we propose in the following to describe its generalization to non simply connected regions.

Let us first consider a simply connected region Ω. In that case [33], the 2-D summation over Ω in EQ.(21) can be replaced by a 1-D summation over the contour of Ω:

$$I_k(\Omega) = \sum_{(x,y)\in C} c(x,y)\ F_k(x,y) \tag{22}$$

where C is the contour of Ω covered counter clockwise and F_k is a preprocessed image obtained with the lines summation of the image s: $F_k(x,y) = \sum_{t=1}^{x} s^k(t,y)$. The coefficient $c(x,y)$ only depends on the positions of its two neighbor pixels on the contour. With the notations of FIG.13,

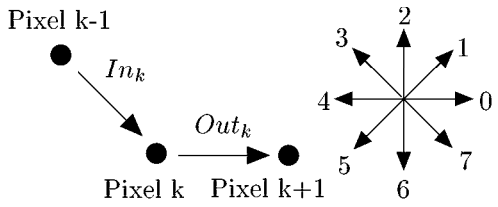

Fig. 13. *Notations used to describe the configuration of 3 consecutive pixels on the contour. If we go along the contour counter-clockwise, In_k and Out_k are the vectors defined with pixel k and its 2 neighboring pixels: the previous one $(k-1)$ and the following one $(k+1)$. The directions of these vectors are encoded with Freeman's code (cf. figure on the right).*

$In_k \setminus Out_k$	0	1	2	3	4	5	6	7
0	0	0	0	0	0	-1	-1	-1
1	1	1	1	1	1	0	0	0
2	1	1	1	1	1	0	0	0
3	1	1	1	1	1	0	0	0
4	0	0	0	0	0	-1	-1	-1
5	0	0	0	0	0	-1	-1	-1
6	0	0	0	0	0	-1	-1	-1
7	0	0	0	0	0	-1	-1	-1

TABLE I

Value $c(x,y)$ of the pixel (x,y), when one goes along the discreet contour counter-clockwise, knowing the position of its 2 neighbor pixels.

$c(x,y)$ is given in TAB.I. See [32] for more details on the way to obtain this values. In particular, we must point out that the partition $\mathbf{w}$ is deduced from the polygonal grid after a translation of the grid by the quantity $(1/2, 1/4)$.

Let us now generalize this technique to non simply connected regions. As shown on FIG.14, a non simply connected region Ω can be broken up in two simply connected regions' families: the full regions $\left(\Omega_i^F\right)_i$ and the hole regions $\left(\Omega_i^H\right)_i$. One can thus write:

$$\begin{aligned} \sum_{\Omega} s^k(x,y) &= \sum_i \left(\sum_{\Omega_i^F} s^k(x,y) \right) \\ &\quad - \sum_j \left(\sum_{\Omega_j^H} s^k(x,y) \right) \end{aligned} \tag{23}$$

Since the regions $\left(\Omega_i^F\right)_i$ and $\left(\Omega_i^H\right)_i$ are simply connected,

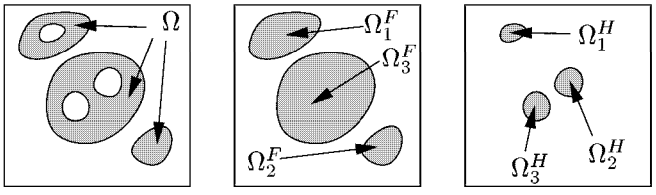

Fig. 14. *Decomposition of the gray region Ω (a) in 2 simply connected region families: the full regions Ω_i^F (b) and the hole regions Ω_i^H (c).*

one can use the contours summation of EQ.(22):

$$\begin{aligned} \sum_{\Omega} s^k(x,y) &= \sum_i \left(\sum_{C_i^F} c(x,y)\ F_k(x,y) \right) \\ &\quad - \sum_j \left(\sum_{C_j^H} c(x,y)\ F_k(x,y) \right) \end{aligned} \tag{24}$$

where C_i^F and C_j^H are the contours of Ω_i^F and Ω_j^H. One can note with this equation that the contribution of a full region has to be considered as positive and the contribution of a hole has to be considered as negative. However, due to the encoding table TAB.I, one can remark that, if a contour of a simply connected region Ω is covered clockwise, the obtained result of the contour summation is the opposite of the result obtained if it is covered counter clockwise as in EQ.(22):

$$\sum_{C\{+\}} c(x,y)\ F_k(x,y) = - \sum_{C\{-\}} c(x,y)\ F_k(x,y) \tag{25}$$

where $C\{+\}$ (resp. $C\{-\}$) is the contour of Ω covered clockwise (resp. counterclockwise). EQ.(24) can thus be written:

$$\begin{aligned} \sum_{\Omega} s^k(x,y) &= \sum_i \left(\sum_{C_i^F\{-\}} c(x,y)\ F_k(x,y) \right) \\ &\quad + \sum_j \left(\sum_{C_j^H\{+\}} c(x,y)\ F_k(x,y) \right) \end{aligned} \tag{26}$$

Furthermore, when a contour is covered with a region Ω on its left, the full regions of Ω are covered counter clockwise and its hole regions are covered clockwise. As a conclusion, one can write:

$$I_k(\Omega) = \sum_{C\{left\}} c(x,y)\ F_k(x,y) \tag{27}$$

with $C\{left\}$ the whole contour of Ω (including full and hole regions) covered with Ω on the left.

So, in order to determine the parameter vector of all the different regions of the image, one can proceed as follow. Let $[A \rightarrow B]$ denote the segment $[AB]$ when going from A to B. Then, let go all over each segment $[AB]$ and compute the contribution of this segment $\sum_{[A \rightarrow B]} c(x,y)\ F_k(x,y)$, $k \in \{0,1\}$. Then, let add this contribution to $I_k(\Omega_{left})$ and let subtract it to $I_k(\Omega_{right})$ where Ω_{left} is the region on the left when one goes from A to B and Ω_{right} the region on the right. Thus, it is possible to determine $I_k(\Omega_r)$ - and so the parameter vector $\widehat{\theta}_r$ - for all the regions Ω_r with examining one and only one time each segment. Moreover, once the parameter vectors of each region has been determined for one grid configuration, they can also be updated very quickly during the optimization process. Indeed, when a node is moved or removed, one only needs to modify the contribution of the segments linked to this node to upload the parameter vector of each neighbor region of the segment.

This approach provides the ability to determine and to update very quickly the parameters of the pdf for each regions' gray levels, even in the presence of non simply connected regions. Using this contour summation thus permits to segment the images of FIG.8 and FIG.2 in respectively 1.3 seconds and 5.8 seconds on a standard PC (Pentium III, 800 MHz).

REFERENCES

[1] European Spatial Agency, "Land and sea ERS-1 applications," in *Workshop ESA on ERS applications ,London*, 1995, vol. br-109.

[2] J. W. Goodman, *Statistical Properties of laser Speckle Patterns*, chapter Laser Speckle and Related Phenomena, pp. 9–75, Springer-Verlag (Topics in Applied Physics Vol. 9), Heidelberg, 1975.

[3] A. C. Bovik, "On detecting edges in speckle imagery," *IEEE Transactions on Acoustics, Speech and Signal Processing*, vol. 36, no. 10, pp. 1618–1627, 1988.

[4] R. Touzi, A. Lopès, and P. Bousquet, "A statistical and geometrical edge detector for SAR images," *IEEE Trans. Geoscience and Remote Sensing*, vol. 26, no. 6, pp. 764–773, 1988.

[5] C. J. Oliver, I. Mc Connell, D. Blacknell, and R. G. White, "Optimum edge detection in SAR," in *Synthetic Aperture Radar and Passive Microwave Imaging*, G. Franceschetti, C. J. Oliver, J. C. Shiue, and S. Tajbakhsh, Eds. 1995, vol. 2584, pp. 152–163, SPIE Proceedings.

[6] O. Germain and Ph. Réfrégier, "On the bias of the Likelihood Ratio edge detector for SAR images," *IEEE Trans. Geoscience and Remote Sensing*, vol. 38, no. 3, pp. 1455–1458, 2000.

[7] R. Fjørtoft, A. Lopès, P. Marthon, and E. Cubero-Castan, "An optimum multiedge detector for SAR image segmentation," *IEEE Trans. Geoscience and Remote Sensing*, vol. 36, no. 3, pp. 793–802, 1998.

[8] R. Cook and I. Mc Connell, "MUM (merge using moments) segmentation for SAR images," in *Conf. on SAR Data Processing for Remote Sensing, Rome, Italy*. SPIE, 1994, vol. 2316, pp. 92–103.

[9] R. G. White, "Change detection in SAR imagery," *Int. Journal of Remote Sensing*, vol. 12, no. 2, pp. 339–360, 1991.

[10] J.J. Gerbrands and E. Backer, "Split and merge segmentation of slar imagery: Segmentation consistency," *IEEE 7th Int. Conf. Pattern Recognition*, vol. 1, no. 21, pp. 284–286, 1984.

[11] S. Geman and D. Geman, "Stochastic relaxation, Gibbs distribution and the Bayesian restoration of images," *IEEE Trans. Pattern Analysis and Machine Intelligence*, vol. 6, pp. 721–741, 1984.

[12] P. A. Kelly, H. Derin, and K. D. Hartt, "Adaptative segmentation of speckled images using a hierarchical random field model," *IEEE Trans. Acoustics, Speech and Signal Processing*, vol. 36, no. 10, pp. 1628–1641, 1988.

[13] E. Rignot and R. Chellappa, "Segmentation of synthetic-aperture-radar complex data," *J. Opt. Soc. Amer. A*, vol. 8, no. 9, pp. 1499–1509, 1991.

[14] P. C. Smits and S. G. Dellepiane, "Synthetic aperture radar image segmentation by a detail preserving markov random field," *IEEE Trans. Geoscience and Remote Sensing*, vol. 35, no. 4, pp. 844–857, 1997.

[15] M. Kass, A. Witkin, and D. Terzopoulos, "Snakes: Active contour models," *International Journal of Computer Vision*, vol. 1, pp. 321–331, 1988.

[16] D. Mumford and J. Shah, "Optimal approximations by piecewise smooth functions and associated variational problems," *Communications on Pure and Applied Mathematics*, vol. 42, pp. 577–684, 1989.

[17] L. D. Cohen, "On active contour models and balloons," *CVGIP: Image Understanding*, vol. 53, no. 2, pp. 211–218, 1991.

[18] R. Malladi, J. Sethian, and B. Venuri, "Shape modelling with front propagation," *IEEE Trans. Pattern Analysis and Machine Intelligence*, vol. 17, pp. 158–175, 1995.

[19] A. Chakraborty, L. H. Staib, and J. S. Duncan, "Deformable boundary finding in medical images by integrating gradient and region information," *IEEE Trans. on Medical Imaging*, vol. 15, no. 6, pp. 859–870, 1996.

[20] V. Caselles, R. Kimmel, and G. Sapiro, "Geodesic active contours," *International Journal of Computer Vision*, vol. 22, no. 1, pp. 61–79, 1997.

[21] Chenyang Xu and Jerry L. Prince, "Snakes, shapes, and gradient vector flow," *IEEE Trans. Image Processing*, vol. 7, pp. 359–369, 1998.

[22] G. Auber and P. Kornprobst, "Mathematical problems in image processing. partial differential equations and the calculus of variations," *Applied Mathematical Sciences, Springer Verlag*, vol. 147, 2001.

[23] R. Goldenberg, R. Kimmel, E. Rivlin, and M. Rudzsky, "Fast geodesic active contours," *IEEE Transactions on Image Processing*, vol. 10, pp. 1467–1475, 2001.

[24] J. Montagnat, H. Delingette, and N. Ayache, "A review of deformable surfaces: topology, geometry and deformation," *Image and Vision Computing*, vol. 19, no. 14, pp. 1023–1040, 2001.

[25] L.H. Staib and J. S. Duncan, "Boundary finding with parametrically deformable contour models," *IEEE Trans. Pattern Anal. and Machine Intell.*, vol. 14, no. 11, pp. 1061–1075, 1992.

[26] C. Kervrann and F. Heitz, "A hierarchical statistical framework for the segmentation of deformable objects in image sequences," *Proc. IEEE Conf. Comp. Vision Pattern Recognition, Seattle*, pp. 724–728, 1994.

[27] G. Storvik, "A Bayesian approach to dynamic contours through stochastic sampling and simulated annealing," *IEEE Trans. Pattern Anal. Machine Intell.*, vol. 16, no. 10, pp. 976–986, 1994.

[28] C. Nguyen, I. Herlin, and C. Graffigne, "A deformable region model using stochastic processes applied to erchadiographic images," in *Conf. on Computer Vision and Pattern Recognition, Urbana Chapagn, USA*. IEEE, 1992.

[29] M. Figueiredo, J. Leitão, and A. K. Jain, "Unsupervised contour representation and estimation using B-splines and a minimum description length criterion," *IEEE Trans. Image Processing*, vol. 9, pp. 1075–1087, 2000.

[30] O. Germain and Ph. Réfrégier, "Optimal snake-based segmentation of a random luminance target on a spatially disjoint background," *Opt. Lett.*, vol. 21, no. 22, pp. 1845–1847, 1996.

[31] S. C. Zhu and A. Yuille, "Region competition: unifying snakes, region growing, and Bayes/MDL for multiband image segmentation," *IEEE Trans. Pattern Analysis and Machine Intelligence*, , no. 9, pp. 884–900, 1996.

[32] O. Germain and Ph. Réfrégier, "Statistical active grid for segmentation refinement," *Pattern Recognition Letters*, vol. 22, no. 3, pp. 1125 –1132, 2001.

[33] C. Chesnaud, Ph. Réfrégier, and V. Boulet, "Statistical region snake-based segmentation adapted to different physical noise models," *IEEE Trans. Pattern Analysis and Machine Intelligence*, vol. 21, no. 11, pp. 1145–1157, 1999.

[34] J. Rissanen, "Modeling by shortest data description," *Automatica*, vol. 14, pp. 465–471, 1978.

[35] J. Rissanen, *Stochastic Complexity in Statistical Inquiry*, World Scientific, Singapore, 1989.

[36] Y.G. Leclerc, "Constructing simple stable descriptions for image partitionning," *Computer Vision*, vol. 3, pp. 73–102, 1989.

[37] T. Kanungo, B. Dom, W. Niblack, and D. Steele, "A fast algorithm for mdl-based multi-band image segmentation," *Proc. Comp. Vision and Patt. Recognition*, vol. CVPR, 1994.

[38] O. Ruch and Ph. Réfrégier, "Minimal complexity segmentation with a polygonal snake adapted to different optical noise models," *Optical Letter*, vol. 22, pp. 1125–1132, 2001.

[39] C. E. Shannon, "A mathematical theory of communication," *Bell Syst. Tech. J.*, vol. 27, pp. 379– 423 ; 623 – 656, 1948.

[40] H. V. Poor, *An introduction to signal detection and estimation*, chapter Elements of hypothesis testing, pp. 5–39, Springer Verlag, New York, 1994.

[41] D. J. Williams and M. Shah, "A fast algorithm for active contours and curvature estimation," *CVGIP: Image Understanding*, vol. 55, no. 1, pp. 14–26, 1992.

[42] E. Jakeman and P. N. Pusey, "A model for non-Rayleigh sea echo," *IEEE Trans. on Antennas and Propagation*, vol. AP-24, no. 6, pp. 806–814, 1976.

[43] E. Jakeman and J. A. Tough, "Generalized K-distribution: a statistical model for weak scattering," *Journal of the Optical Society of America A*, vol. 4, no. 9, pp. 1764–1772, 1987.

[44] J. K. Jao, "Amplitude distribution of composite terrain radar clutter and the K-distribution," *IEEE Trans. on Antennas and Propagation*, vol. AP-32, no. 10, pp. 1049–1062, 1984.

Frédéric Galland is graduated from Ecole Nationale Supérieure de Physique de Marseille (ENSPM) in 2001. He is currently a PhD student in the Physique and Image Processing Laboratory of Fresnel Institut (UMR CNRS 6133) and ENSPM. His main research interests include image segmentation and statistical techniques.

Nicolas Bertaux is an assistant professor in Electrical Engineering at Ecole Nationale Supérieure de Physique de Marseille. He gradu-

ated from the Ecole Normale Supérieure of Cachan. He received the M.Sc degree in Electrical Engineering from Paris University (Orsay) in 1993, and the "Agregation degree" in Electrical Engineering in 1994. He received a Ph.D. degree from Paris University in January 2000 in Electrical Engineering. His present main research interests in Institut Fresnel (UMR CNRS 6133) include digital image processing and signal processing.

Philippe Réfrégier is a full professor of signal processing at Ecole Nationale Supérieure de Physique de Marseille. He graduated from Ecole Supérieure de Physique et Chimie Industrielles de la ville de Paris in 1984 and he received a PhD in solid state Physics in 1987 from the University of Paris Orsay. From 1987 to 1994, he was a member of the Laboratoire Central de Recherches of Thomson-CSF in Orsay. His present research interests in Institut Fresnel (UMR CNRS 6133) include digital image and signal processing, pattern recognition, optical information processing and statistical optics. He is the editor of several books and proceedings, presently topical editor of *Applied Optics, Information Processing*, the author of books and of more than 80 refereed articles in international scientific journals. He organized and participated to different international conferences.